Experiments and simulations of sitting classification for wind and temperature observation

GUO Jianxia[1], GUAN Yanhua[2], SHEN Xuefeng[3], GUO Jiangfeng[4], TANG Zhiya[5], TIAN Dongxia[1], XUE Zhengzheng[1], CHEN Ting[1], MAO Jiajia[1] and YOU Yuan[1]

1. Meteorological Observation Center of CMA, Beijing,China
2. Hebei Province Meteorological Bureau, Shijiazhuang, China
3. Zhejiang Province Meteorological Bureau, Hangzhou, China
4. Shanxi Province Meteorological Bureau, Xian, China
5. Chengdu University of Information Technology,Chengdu, China

Tel. 86-10-68407934 Fax. 86-10-68400936 E-mail: gjxaoc@cma.gov.cn

ABSTRACT

To evaluate the influence of the environs to the measurements of wind and temperature, a series of field experiments have been done in china from 2012 to 2014. Meanwhile two types of numerical models have been used to simulate the conditions of the experiments. This paper presents the design of the experiments, as well as some observation facts from the experiments, and the comparison of the results between the experiments and the simulations. Then some standards of sitting classification for temperature and wind observing were evaluated by a set of sensitive simulation. The results show that more than 30% attenuation is observed at 10 times away from the obstacle height, and over 80% attenuation at 5 times away from the obstacle height. The requirements of distance height ratio will be decrease with the increase of the height or thickness of obstacles and the decrease of the wide angle of obstacles. The impacts of water body or the arterial road on temperature will be observed more significant when the wind speed is 2 m/s, and the influence distance will be more than 100m.

Key words: sitting classification, temperature, wind, observation experiments, simulations

Text

1. Introduction

Instrument exposure environment has certain impacts on representativeness, accuracy, and comparability of meteorological observation data, and this kind of influence is usually larger than the error limit of observing instruments. To avoid such impacts, *CIMO GUID* (2010) releases the judgment standards and requirements to the environmental grades for the weather elements being observed at meteorological stations. Through observation experiments and numerical simulation, this paper is to study and discuss the environmental grades and standards for wind and temperature observation in the *CIMO GUID*.

2. Observational experiment design

We design 4 experiments, one of them is for wind observation, and the others are for temperature observation. In detail, the first experiment is for the impacts of obstacle on wind speed and direction, the second to four are for the impacts of water body, surface heat source and arterial road on temperature, respectively. The following is the brief description to the design scheme of the experiments.

Experiment I: Impact test of single building on wind speed and direction

This experiment is carried out on the vast and open grassland in the suburb of Guyuan, Hebei province China, located in the place of 41°37′ N, 115°26′ E ,where northwest wind blows in winter while south wind prevails in summer. This test is designed mainly for northwest wind and south wind. The layout and real photos are shown in Figure 1.

Figure 1 Layout and real photos of the wind observation impact test in Guyuan, Hebei

In the center of the test area, a single building in the direction of southwest to northeast is designed with 50 m long, 3 m wide and 15 m high. Seven automatic weather stations (AWSs) for observing wind speed and direction are fixed at the spots of 45 m, 75 m, 120 m, 150m, 225m and 300 m along the vertical centerline on the southeast side of the building, 4 AWSs at the spots of 15 m, 45 m, 75 m and 120 m along the extended north line in the north side of the building and another 4 AWSs at the spots of 75 m, 120 m, 150 m and 300 m along the extended line in the direction of 45°,which in the angle of 12.5° with the building. At the spot 300 m away from the building in west, one wind speed and direction observation AWS is set up to act as a reference station in which temperature observation is designed at the 2 m and 9 m layers. The test was started on August 16, 2012. First the 16 AWSs were installed in the designed positions and coincident observations were tried. Establishment of the building began on September 6 and ended on December 2 in the center of the test area. This test provided the quantitative observation data of every observing spot on the lee side of obstacle which was affected by buildings under the condition of vertical and 45° inflow airs.

Experiment II: Impact test of water body on temperature observation

The experiment field is in Qianmudang, Haiyan County, Zhejiang Province China, located in the place of 30°33′ N, 120°50′ E with altitude of 5 m or so. The area is 4.83 km^2 large in which 1.27

km^2 area is waters whose average depth is 3 m. The winter dominant wind in this place is northwest wind. Five temperature and humidity AWSs are set up respectively at the spots of 0 m, 50 m, 100 m, 200 m and 300 m along the line in the southeast side of the waters. At the 100 m and 150 m spots in the upwind direction of the northwest side of the waters two reference stations are built. The test layout and scheme are shown in Figure 2.

Figure 2 The layout of Qianmudang water test in Zhejiang

Almost all the area around the waters is covered by farmland where the same kind of crops is cultivated during the planting seasons. The observation was carried out from January 1 to 30 May, 2012, when there were no crops during January and February in the farmland but from March to May spring wheat grew up gradually. The purpose of this experiment is to obtain the quantitative observation result of the impact of water body on the temperature in the downwind direction.

Experiment III: Impact test of surface heat source on temperature observation

The experiment field is located at the place of 30°35' N and 103°59' E, within a university of Chengdu, Sichuan Province China. The inner area of the field is 40×80 m, covered with grass. A 3-floor office building is 30 m away from the east edge of the field, and a one-floor building is about 40 m away from its north edge. Some trees and bamboos about 5 m tall are growing at 15m away from the west edge of the field. Six temperature and humidity observing AWSs are set up in the field. The layout and real photo are shown in Figure 3.

Figure 3 The layout and real photo of impact test of surface heat source in Chengdu

According to the classification standards of temperature and humidity observation grades given in *CIMO GUID*, the heat source area proportions at the circles with the radius of 100 m, 30 m and 10 m are calculated at every site. The grades of the 6 AWSs are determined, as shown in Table 1.

Table 1 The heat source area proportions and grades at different test sites in Chengdu

Sites	100 m	30 m	10 m	Grades
1	31%	0	0	2
2	29%	7%	0	2
3	32%	11%	0	3
4	23%	29%	5%	3
5	25%	32%	16%	4
6	28%	22%	22%	4

The observation test began from February 21, 2014. First of all, all the sensors were put into one instrument shelter, doing coincident observation and comparing the differences of these instruments. On March 12, 2014, the coincident observation was finished. Then, the sensors were separately placed into their own shelters, and the observation test started formally. This experiment is to measure the differences of temperature observations which were done at stations in different grades.

Experiment IV: Impact test of arterial road on temperature observation

One national road in Shaanxi Province, China, is selected to do the observation test of arterial road impact. The test road is located in 35°9'N and 110° 7' E, north-south direction and 10 m wide, with daily mean traffic volume of 4,350. By both sides of the road are farmlands where no crops grow in winter, but in spring and autumn the spring wheat and corns are planted respectively. On the east side of the national road, 8 sets of temperature observation AWS are set up at the spots being 15 m, 30 m, 50 m, 75 m, 100 m, 125 m, 150 m and 200 m away from the road, of which at the 30 m spot a sensor for measuring wind speed and direction is fixed at the same time. The experiment layout and real photo are shown in Figure 4.

Figure 4 The layout and real photo of the road test in Shaanxi

The experiment began on January 2, 2014 and ended on April 8. After the test, the 8 sets of temperature sensors were put into one shelter to do the coincident observation which lasted for 16 days from April 9 to 24, 2014.

3. Experiment result analysis

3.1 Observation result of impact of single building on wind speed and direction

First of all, the coincident observation data collected before the building was established from August 16 to September 6 are analysed. Figure 5 shows the variation of the wind speed and direction difference between the 15 AWS and the reference AWS, which changes along with the wind speed at the reference site. The horizontal axis represents the wind speed at the reference site while the ordinate shows the difference of wind speeds of every station and the reference station as well as the wind direction difference between them. It is seen from the figure that wind speed difference mainly concentrates in the range of ±2 m/s (Figure 5a), which means that the wind speeds observed from every station are more consistent. The wind direction difference is bigger when the background wind is <2m/s (Figure 5b) or some even get up to ±180°, but when the background wind is > 2m/s, the wind directions of these station are highly consistent. This phenomenon indicates that in the case of slow wind speed the airs are in turbulent flows while in the time of fast speed they are stratified flows. Given this, this paper is to take the samples >2 m/s to analyse the effect of buildings.

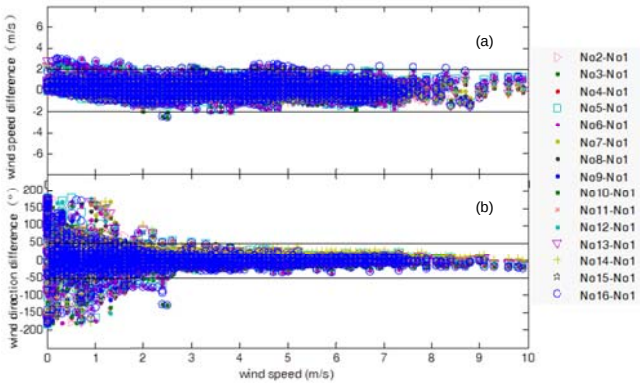

Figure 5 Variation of wind speed and direction differences between Site 2-15 and Site 1 before establishing the building along with the wind speed at Site 1

The building was completed on December 2, 2012. Site 2-8 were set up at the lee side of northwest wind and site 9-16 were in the lee side of south wind. Figure 6 reveals the variation of wind speed and direction difference between site 2-8 and the reference site (site 1) associated with the change of wind speed at the site 1. Figure 6a shows that the wind speed difference of site 2-6 is negative, which denotes that the wind speed is reduced after the airflow passes the obstacles. The speeds at site 2 and 3 have the largest velocity deficit, site 7-8 which stand at the far and see the

smallest reduction amplitude from beginning to end, and site 2-6 experience the gradual increase in attenuation along with the increase of the background wind speed.

Figure 6b shows the wind direction measured at Site 2, which is the nearest to the building, is disturbed most violently and there appear winds in all directions, having a high proportion of samples which are in the opposite direction to the northwest wind. The wind direction deviations of Site 3 are mostly concentrated in the range of ±40°, those of Site 4 are within ±30°, of Site 5 and 6 in ±15°, and of Site 7 and 8 in ±10°. With the increase of wind speed, the wind direction deviation between Site 2 and the reference station shifts toward ±180° while the deviations between Sites 3-8 and the reference station is gradually decreasing, getting to the part near 0°. The absolute values of the average deviation of wind directions measured at Sites 2-8 are 137°, 19°, 11°, 8°, 6°, 5° and 4°in sequence. It is thus evident that the building impact on wind direction behind Site 5 (120 m, 6 times the height of the building) is not significant.

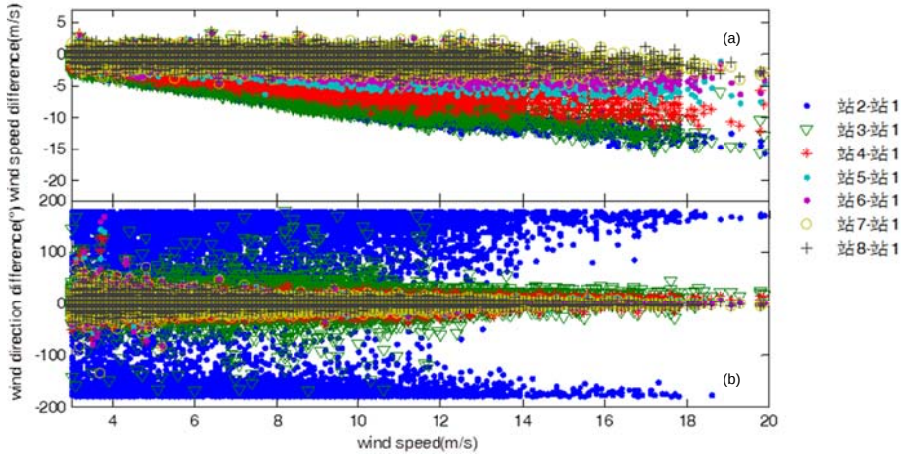

Figure 6 Variation of wind speed and direction difference between Sites 2-8 and Site 1 in time of northwest wind associated with the change of wind speed at Site 1

(a) Wind speed difference (b) Wind direction difference

Figure 7 sums up the mean attenuation rate of Sites 2-8 under various wind speed conditions at 1 m/s interval. It is seen from the figure that all the sites agreeably reveal the attenuation proportion in fast wind speed background is larger than that in slower wind speed background. Being<=150 m (10H, H represents the height of obstacle) away from the building, the mean attenuation proportion of wind speed of 11 m/s is the biggest, reach to 30% at 10H; being further away from the building, the mean attenuation proportion of every wind speed is <10%. When the background wind speed is <3m/s, the wind speed attenuation of the lee side of obstacle reduces along with the increasing distances, and the attenuation proportion becomes the biggest at the 45 m spot (3H) getting up to 30%-60%, at the 10H spot being 0%-15%, and at 15H spot approaching 0%. When the background wind speed is >3 m/s, the attenuation proportion of wind speed at every spot in the lee side increases first and then decreases with the 5H spot having the biggest rate, getting up to 65%-80%,

and the 10H spot averagely reducing 20%-30%. However, the attenuation proportions for the spot being15H or further away basically maintain within 10%.

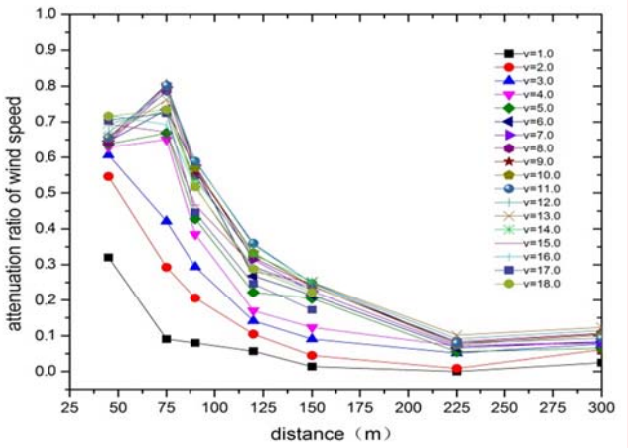

Figure 7 Average attenuation proportion under every wind speed condition at sites 2-8 in northwest wind

Figure 8 reveals the variation of wind speed and direction deviation between sites 9-16 and site 1 in time of south wind along with the change of wind speed at site 1. At this condition, the angle between airflow direction and the building is 45°. We can see from the Figure 8(a) that site 9, located most closely to the building, always has the biggest attenuation. Following it, are site 16 at the 75 m spot and site 12 at the 120 m spot in 12.5° direction, and then is site 10 at the 45 m spot in 45° direction. Site 11 and 13 in 45° direction and site 14 and 15 in 45° direction do not have notable reductions in wind speed, and when wind speed is large there are some samples of wind speed increasing. By comparing site 11 with site 16, and site 13 with site 12, we can clearly see the attenuation in 12.5° direction is larger than in 45° direction, which suggests that when the inflow wind is at 45° angle to buildings, its wake flow is not in the 45° direction but clockwise shifts to the 12.5° direction.

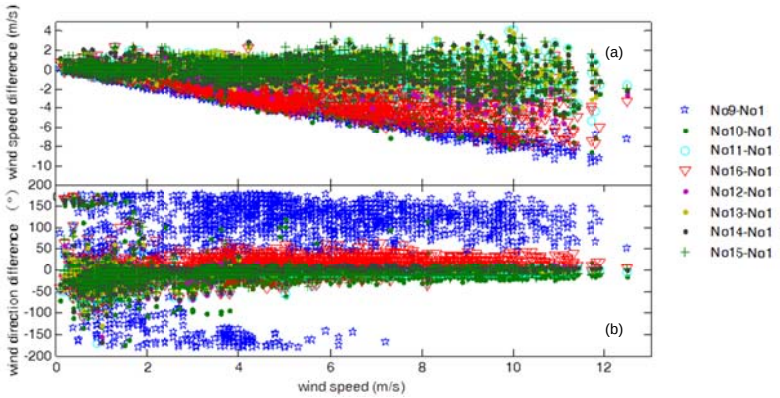

Figure 8 Variation of wind speed and direction difference between site 9-16 and site 1 in south wind along with the change of wind speed at site 1

From Figure 8b, we can see that the site 9 appears the most remarkable direction deviation, which focus on the clockwise 50° to 180°. Site 16 deviated within 50° of clockwise. On the contrary, site 10 deviated within 50° of anticlockwise. The wind deviation of rest site is not obvious.

3.2 Observation results of water body impact on temperature

Figure 2 shows the serial number of every AWS adopted in the water observation test. When it blows northwest wind sites 1-5, which are respectively at the spots of 0 m, 50 m, 100 m, 200 m and 300 m, are in downwind direction of the water body, and sites 6-7 are reference stations in the upwind direction. Figure 9 displays the monthly mean difference between sites 1-5 and site 6 during the observation period. From the figure we can see that sites 1-4 have clearly recorded the impact of water body on the temperature drop in day time and temperature rise over night in the surrounding environment, and, moreover, the closer to the adjacent water body, the more obvious the impact is. Being away from the water, the impact gets weakened. Site 4, which is 200 m away from the water body, can observe obvious increase in temperature at night. With respect to the effect of lowering temperature of the water body during the day, sites 1-3 can observe the phenomenon more clearly but sites 4-5 cannot catch notable data during the test period. So, it is evident that the impact of water body mainly is on the temperature increase during the night time, and the impact range can be 200 m away in winter. In spring, however, the impact range is diminished.

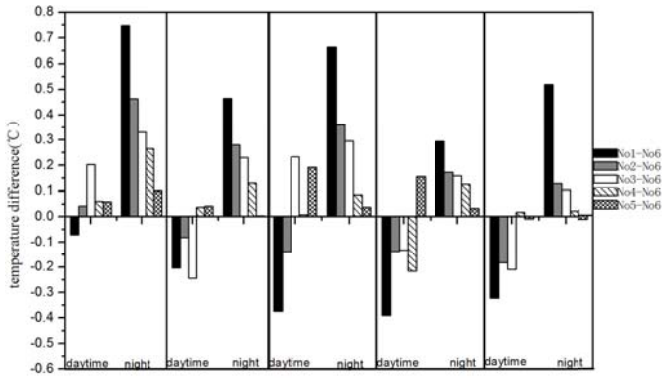

Figure 9 Variation of mean temperature difference between sites 1-5 and site 6 in time of northwest wind across water body

Figure 10 shows the variation of the temperature difference between sites 1-5 and site 6 when northwest wind blows over day and night along with the change of wind speed. It is seen from the figure that the temperature increase effect of waters over night is more significant under the environmental condition with wind speed <3 m/s, and when the wind is >3 m/s, the effect of waters on night temperature increase is not noticeable. The impact of waters on temperature decrease during the day time is not closely related to wind speed.

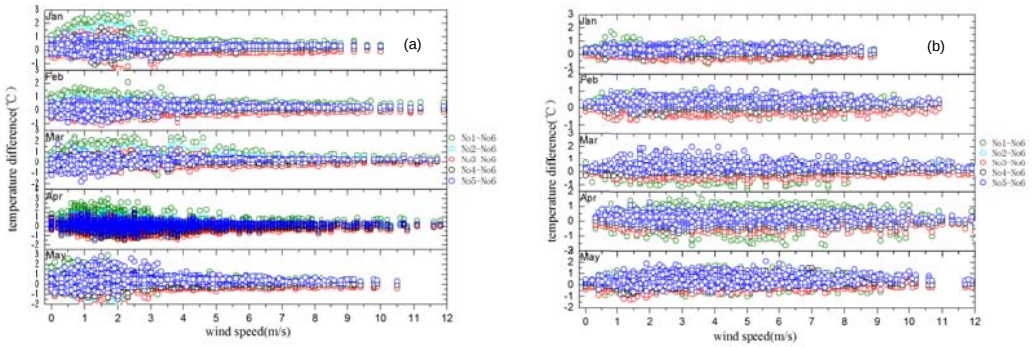

Figure 10 Variation of temperature difference between sites 1-5 and site 6 over night (a) and day (b) in northwest wind along with the change of wind speed

3.3 Observation result of impact of surface heat source on temperature

Based on the laboratory calibration data and the consistent observation data in the field, we calculated the errors of instruments and corrected the errors of the observation data. Figure 11 shows the daily average variation of temperature difference between the observing sites and site 2 in Chengdu test field. It is seen that the temperature difference is significant during the two periods of 0:00-8:00 BT and 13:00-17:00 BT, especially for site 6 and 2 it is more significant and the day maximum difference appears at 15:00 BT getting up to 0.28°C, and the night maximum difference can also be 0.25°C in 2:00-4:00 BT. The temperature difference between site 5 and 2 can be 0.2°C at night and 0.15°C in the day. Site 4 and 2 have bigger temperature difference in 13:00-17:00 than in other period of time, reaching 0.15°C, similar to that of site 5, and the temperature difference and characteristics of other periods are similar to site 1 and 3 with magnitude being about 0.05°C.

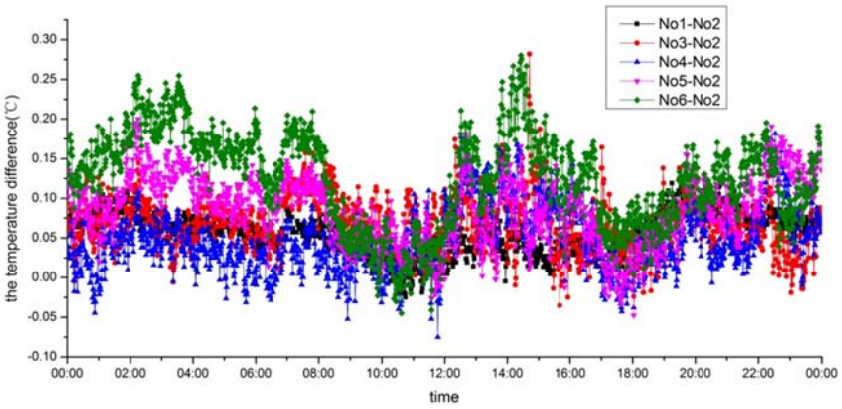

Figure 11 Daily mean variation of temperature difference between Sites 2-6 and Site 1 in Chengdu experiment

Due to the different areas and locations of heat sources in every station, wind direction is not taken into account here. Therefore, the temperature differences between sites 1, 3, 4 and site 2 are not so great, but sites 5-6 at Grade 4 have obviously higher temperature than the other sites in Grade 2-3, and site 4, which belongs to Grade 3, also has higher temperature in the afternoon than sites 1-2 of Grade 2. It is thus seen that the higher the grade is, the more obvious the heating effect of temperature is. In the period 8:00-12:00 BT after sunrise and the period 17:00-20:00 BT after sunset

the atmospheric turbulent flows play actively and atmospheric stratifications change, so the temperature difference between the observing sites are not so clear.

3.4 Observation results of impact of arterial road on temperature

After the data is pre-processed based on the coincident observations, the daily variations of temperature differences between sites 1-6 and the reference station (site 7) in time of west wind are summed up (Figure 13). From the figure it can be seen remarkably that in the 9:00-17:00 daytime the temperature difference between sites 1-5 and site 7 is positive, and the deviation values decrease gradually from site 1 to site 5, of which the biggest deviation of site 1 is 0.2℃ and that of site 5 is 0.08℃. Between midnight and dawn the temperature of site 1 drops greatly, especially before the sunrise with deviation getting to -0.14℃, the most sharply. The decrease in temperature at site 2 is just next to site 1 with 0.08℃ down. This observation result indicates that after sunrise in the daytime solar radiation makes roads warm, where temperature rises up with degrees higher than in crop fields and naked earth. At the same time, traffic volume is very large and the increasing emission of the exhaust gases cause the observation site near roads to be impacted by the heat source and temperature increase is enhanced. Such kind of temperature increase effect declines with the growth of the distance to road, and by the spot 100 m (site 5) only weak increase in temperature is observed. At night, however, solar radiation cools down and the extent of radiation cooling on roads is larger than in crop fields. Meanwhile, traffic flows over night are very small, almost having no exhaust gas emission, so the night road becomes a cold source. The observing sites near roads are affected by the temperature change on roads, having the record of drop in temperature. Such kind of temperature decrease effect can only extends 30 m, indicating that the intensity of the night cold source is much weaker than the intensity of the heat source during the day time.

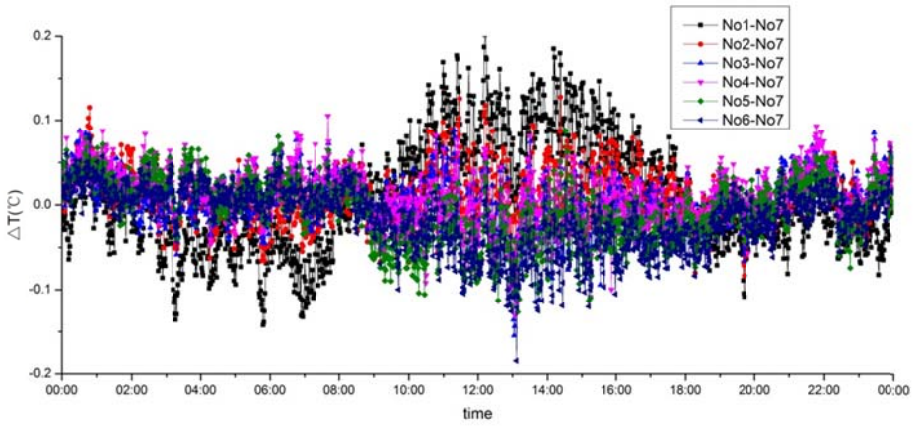

Figure 12 Daily mean variation of temperature difference between sites 1-6 and site 7 in Shaanxi road experiment

4. Numerical simulation evaluation

4.1 Simulation evaluation on requirement of distance to the obstacles for wind observation

Utilizing Fluent, Computational Fluid Dynamics software, the impact of building on wind is simulated and evaluated. First, the model is tested with observation data from experiment I. A building with the same size of the building in test field was established in the model. The computational domain is 40H×20H×5H (H refer to the height of the building of 15 m), the inflow border is 10H away from the building and the outflow border is 30H away. It is hexahedral structure grid, having 2,170,000 grids approximately.

Figure 13 compares the observations of vertical lee side of northwest wind and southerly lee side in the directions of 45° and 12.5° with the model simulation results. From the figure, we see that the simulation result of the lee side of northwest wind is smaller than observations, but the results at the southerly lee side in the directions of 45° and 12.5° are in better agreement with the observations.

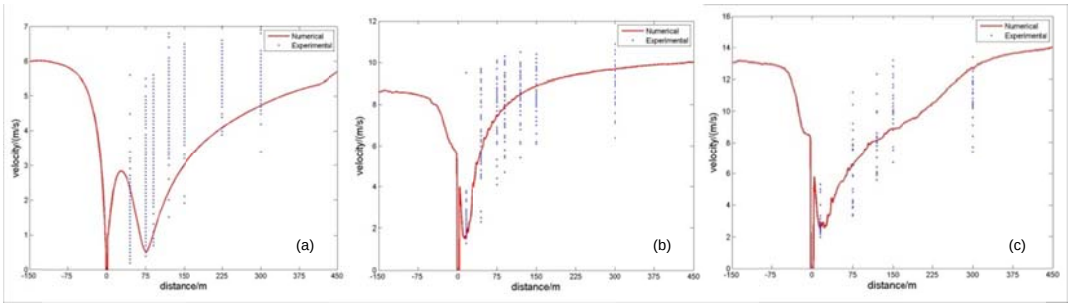

Figure 13 Comparison of simulation and observations from Hebei Guyuan building experiment

(a)northwest wind in the vertical centreline of the building

(b)south wind in the line of 45° angle with the building

(c)south wind in the line of 12.5° angle with the building

4.1.1 Impact range simulation of wind speed

Figure 14 is a speed ratio figure (speed ratio = wind speed in the simulation area/ coming wind speed at the same height),in which the wind speed is 6.0 m/s, the coming wind is vertical (Figure 14a) or at 45° angle to the building (Figure 14b), and z=10 m. Supposing that the impacted area is with speed ratio ＜0.9 or ＞1.1. It is seen from the figure that when airflow is vertical to obstacles, the impacted area is mainly concentrated in the range of 10H (H is the height of building). In the area 10 times farther away, there is long and narrow wake section, extending to 28.5H. In addition, influenced by the inverse flow, the windward side in the range of 3H also has obvious fading parts. When the airflow and building have 45° angle, all the impacted areas in front of and behind the building get enlarged, and the wake part passes 30H. According to the CIMO standard of wind observation grade, the 30H, 10H, 5H and 2.5H spots corresponding to 1-4 grade stations, the maximum attenuation ratios are 5%, 45.8%, 88.3% and 55.8% respectively in case of vertical coming flows, and are 18.2%, 45.3%, 64.0% and 88.0% respectively when it is 45° angle wind. Therefore, it is seen that for the 3-4 grade stations the maximum error of wind speed can reach 88%

or more. The observation data reveals that the average attenuation ratio is 75% when at the 5H spot wind speed is 6m/s, being close to the simulation result, and at the 10H spot the average attenuation ratio is 20%, smaller than the simulation result.

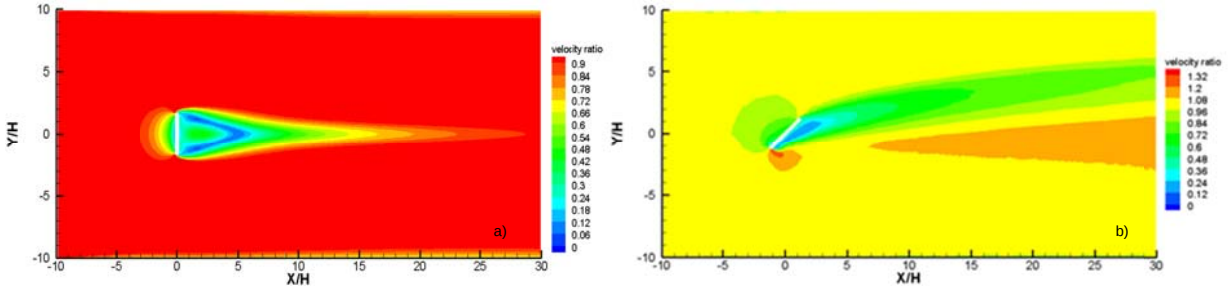

Figure 14 Horizontal cross-section speed ratio, z=10 m

a) vertical coming wind b) 45° angle wind

4.1.2 Impact range simulation of wind direction

Figure 15 shows the 10 m height wind direction deviation between the direction and the coming wind direction (taking the absolute value). Supposing that the area where the deviation is bigger than 10° is the affected area. It is seen from the figure that in time of vertical coming wind, the wind directions in the range of 7H on lee side of the building are affected, but the area impacted by windward wind direction distributes toward the two ends in a symmetrical pattern, and the extending range is about 1.5H. At the moment of 45° angle coming wind, the affected range on the lee side of the building grows to 16H, and at the same time the affected range deflects about 12.5° towards the coming wind direction of wind speed. For the nearby buildings, the backflow area impacted by eddy diminishes obviously, and the impact range of the area with windward side deflecting to coming flow expands, but decreases to other directions.

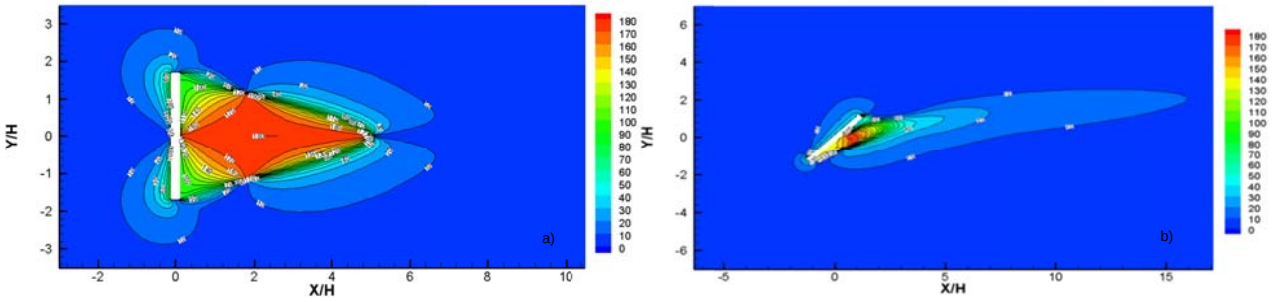

Figure 15 Deviation of horizontal cross-section wind direction, z=10m

a) vertical coming wind b) 45° angle coming wind

4.1.3 Sensitivity analysis

We design 4 groups simulation schemes and carry out the sensitivity analysis respectively on the wind speed of coming flow and the geometrical features (height, thickness and wide angle) of the building (Table 2).

Table 2 Simulation schemes

Basic condition	Group I	Group II	Group III	Group IV
Building size: 50m*3m*15m Coming wind speed: 6m/s Coming wind direction: Vertical to obstacle	Coming wind speed: 4m/s, 6m/s, 8m/s,11m/s, Others: basic conditions	Building height: 3m, 6m, 9m, 12m, 15m, Others: basic conditions	Building thickness: 3m, 25m, 50m, Others: basic conditions	Building length of windward side: 6m, 18m, 36m, 50m Others: basic conditions

The sensitive simulation results of each group is shown in Figure 16. Figure 16(a) reveals that the distance height ratio for wind speed return to 90% in the lee side of building increases along with the increase of coming wind speed, and the reattachment points also move backward along with the increasing wind speed. The attenuation proportions of CIMO 1-4 grade stations are given in Table 3. The 5H spot of Grade 2 is in the cavity area, so its attenuation proportion is the maximum in various wind speed conditions. At the 2.5H sport of Grade 4 station, the attenuation proportion of 4-6 m/s coming airflow is higher than that at 10H spot of Grade 2 station, and the attenuation proportion of 8-11 m/s coming airflow is lower than that at 10 H spot. The 30H spot of Grade 1 station does not get obvious influences when 4-6 m/s airflow blows but in time of 8-11 m/s coming airflow the attenuation occurs, exceeding 10%.

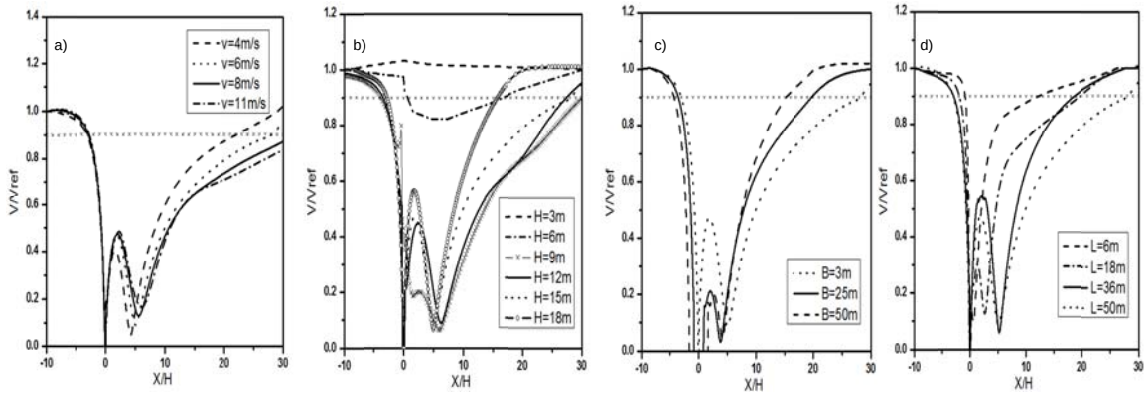

Figure 16 Variations of speed ratio along with the vertical centerline of the building

a) sensitive to the coming flow; b) sensitive to the building height;

c) sensitive to the building thickness; d) sensitive to the building length.

Table 3 Attenuation proportions of 1-4 grade stations under different wind speed

Wind speed (m/s)	30H	10H	5H	2.5H
4	0	40%	87.5%	68%
6	5%	45.8%	88.3%	55.8%
8	12.5%	52.5%	81.2%	47.5%
11	16.8%	55.4	88.8%	44.4%

Figure 16(b) shows that when the height of building is 3 m, wind speed observation does not have any influence, and wind speed attenuation of the lee side of the 6 m building is 15.8% at most, located at 5.8H spot. When building is taller than 9 m, its lee side sees violent wave motion of wind and the range of 10H is affected greatly. Going along with the increase of building height, the requirement to distance height ratio that returns to 90% coming airflow diminishes. With such coming wind speeds, the 30H spot of Grade 1 station can basically return to over 90%; the 10H spot of Grade 2 station can separately return to 62%, 59.2%, 49.2% and 34.5% of the coming airflow on the lee side of the building at 18 m, 15 m, 12 m and 9 m height; the 5H spot of Grade 3 station can respectively return to 6.9%, 11.7%, 8.7% and 8.8% of the coming airflow; and the 2.5H spot of Grade 4 station can separately return to 50%, 44.2%, 37.7% and 19%. These simulation results mean that for buildings in the height of 9-20 m, the requirement of distance height ratio to the 2-4 grade stations should be higher than the CIMO standard.

Figure 16 (c) suggests that the distance height ratio that returns to 90% coming airflow is respectively 28.5H, 19.9H and 15.1H on the lee side of buildings with thickness of 3 m, 25 m and 50 m. So, we see that for thick buildings the requirement to distance height ratio on the lee side can be lowered a little.

Figure 16(d) demonstrates the impact range of buildings with different lengths on lee side wind speeds. Table 4 lists the wide angles and attenuation proportions of wind speeds corresponding to the spots at 2.5H, 5H, 10H, 20H and 30H respectively. From the figure and table we can see that with the increase of the length of buildings, the backflow area of the windward side expands, meanwhile the scope of cavity wake area of building lee side expands as well. For the obstacles having 10° wide angle, there are ＞42% errors at the 2.5H spot, ＞50% errors at the 5H spot, ＞26% errors at the 10H spot, ＞21% errors at the 20H spot and ＜10% errors at the 30H spot.

Table 4 Wide angles and attenuation proportions of lee side wind speed in different building widths

Distance /m L/m	2.5H		5H		10H		20H		30H	
	Wide angle(°)	Attenuation Proportion %	Wide angle(°)	Attenuation Proportion %	Wide angle(°)	Attenuation Proportion %	Wide angle(°)	Attenuation Proportion %	Wide angle(°)	Attenuation Proportion %
6	9.1	41.7	4.6	20.5	2.3	12.3	1.1	5.5	0.7	0.0
18	25.0	86.7	8.5	45.0	6.8	25.2	3.4	8.5	2.3	0.0
36	40.5	46.7	25.0	92.3	13.6	36.5	6.9	10.5	4.6	0.0
50	79.6	55.8	32.2	88.3	18.8	45.8	9.5	20.8	6.4	5.0

4.2 Simulation evaluation on temperature standard

4.2.1 Road impact simulation

Road impact is simulated by using the Urban Sub-domain Scale Model (USSM). The model is first tested with the observation data of experiment IV. Figure 17 shows the comparison of the simulated and observed temperatures at 16:00 BT January 27. It is seen that the USSM can better simulate the temperature difference which is caused by road heat sources.

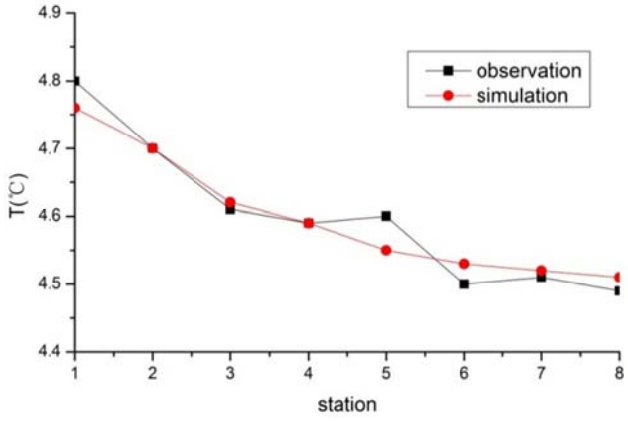

Figure 17 Comparison of temperature observed in Shaanxi road experiment and the simulation value from USSM

By utilizing USSM further, sensitivity numerical simulation for with/without road or increasing width of road is conducted on Shaanxi experiment site. Figure 18 shows the distribution of the temperature difference between with and without road in time of 2 m/s west wind. It is seen that the existing road causes the temperature in 100 m range on its eastern side to rise up more than 0.1℃, and in 140 m range to rise up 0.05℃. The 100 m temperature standard for Grade 1 station in CIMO GUID can meet the error requirement of 0.1℃.

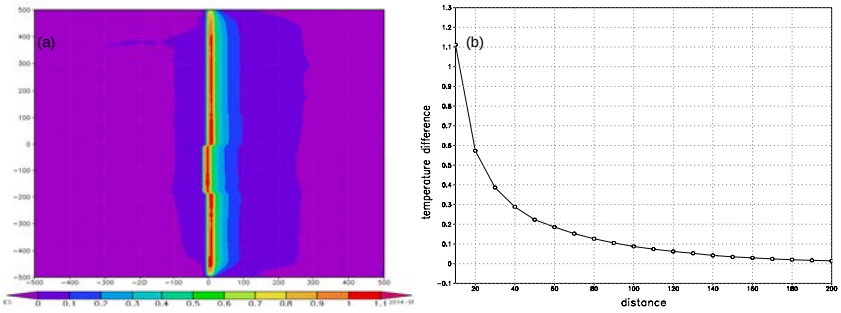

Figure 18 Distribution of temperature differences between with and without road

(a) Regional plane distribution, (b) temperature difference curve along the axial line of testing point

Figure 19 displays the result of a set of sensitivity simulation test countering background wind speeds, which are 0.5 m/s, 1 m/s, 2 m/s, 3 m/s, 5 m/s, 8 m/s and 12 m/s respectively. In the figure the distance with 0.1℃ temperature difference between with and without road is shown. From the figure we can see that under the background of light wind speed the impact of roads is larger than that seen in the background of high wind. When wind blows at 2 m/s speed, the impact scope of roads is the biggest, getting up to 100 m, when it is at 0.5 m/s speed the impact scope of roads can be 60 m, but when it is 12 m/s the impact scope of roads is only 30 m.

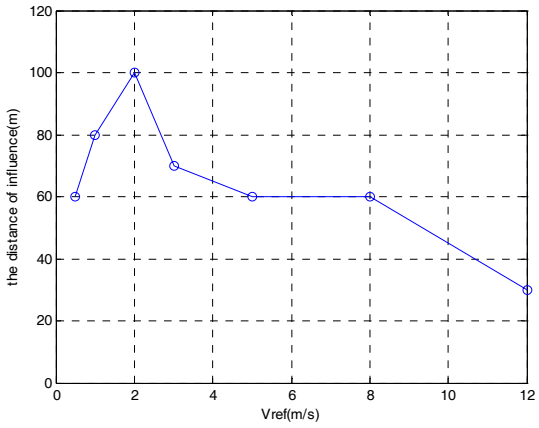

Figure 19 Simulation result of road impact range changing with wind speed

Figure 20 shows a set of sensitivity test for road width, the background wind speed is 2 m/s and the road widths are 10 m and 30 m respectively. It is seen from the figure that when road width increases the impact scope of roads on temperature expands. The 0.1℃ range extends to 120 m, the 0.05℃ range extends to 160 m and then the impact quickly decreases, and by the spot extending to 200 m there is no any effect, the same as on the 10 m wide road.

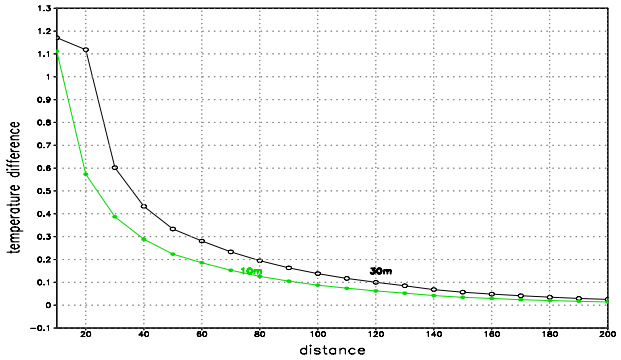

Figure 20 Contrast of sensitivity results with/without 10 m and 30 m wide roads

4.2.2 Water body impact simulation

The water body impact is simulated further by using USSM. First the model is tested with observation data of experiment II. Figure 21 shows the model surface and the comparison between the simulated temperature and observed temperature. It is thus seen that USSM can better simulate the temperature difference generated by water body.

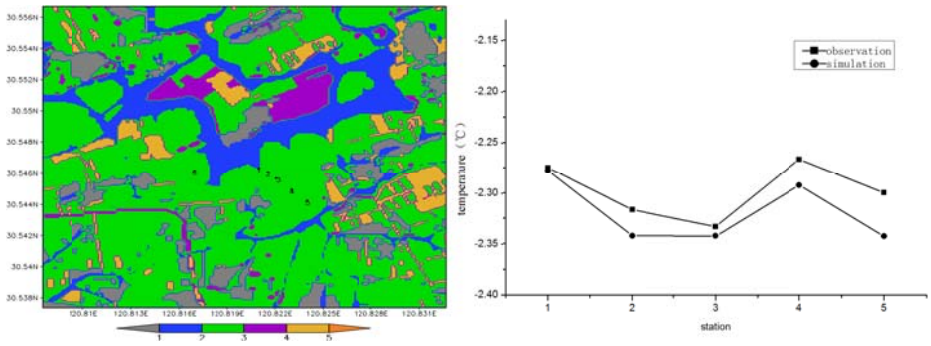

Figure 21 Model surface and the comparison of simulation and observation in experiment II

a) Model surface b)the temperature of simulation and observation at 22:00BT, January 25

The USSM is further used to conduct the sensitivity numerical simulation with/without the water body. Figure 22 gives the distribution of temperature difference between with and without water body at noon 12:00 BT and night 2:00 BT January 25. From the figure, we see that during the daytime the water body can lower temperature 0.05-0.1℃ to the downwind direction in the range of 100-200 m, 0.1−0.7℃ in the range of 50-100 m and >0.7℃ within 50 m. At night water body can increase temperature 0.05-0.1℃ to the downwind direction in the range of 50-200 m, and 0.1-0.3℃ within 50 m.

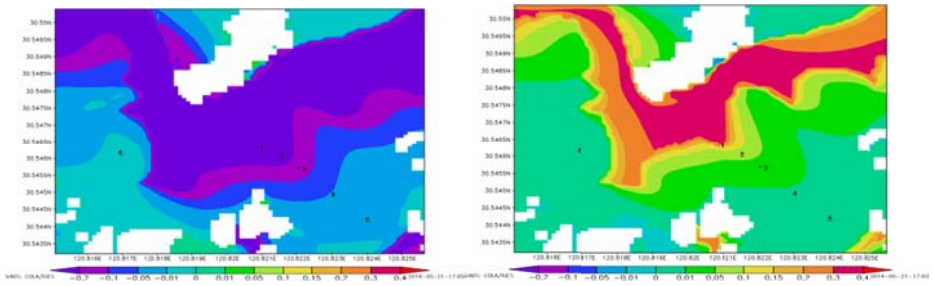

Figure 22 Distribution of simulation temperature difference between with and without the water body in Zhejiang test

a)12:00 BT, January 25 b) 2:00 BT, January 25

5. Conclusions

This paper designed the observation experiments and numerical simulation experiments aiming at the impact factors on wind and temperature observations. The results suggest that:

(1) Numerical simulation and observation experiment both indicate the impact of building on high

wind is more significant than on light wind; its impact scope on inclined airflow is larger than on vertical flow; the impact range on wind speed is larger than on wind direction. The 5H spot on the building has obvious cavity area, having the biggest influence on wind speed. At the 10H spot the observed wind speed error is higher than 30%, and the simulated error even exceeds 50%.

(2) Simulation suggests that when the height and thickness of obstacles increase and the wide angle decreases, the requirement to corresponding distance height ratio declines. For the 9-20 m obstacles, the requirement to distance height ratio of the 2-4 grade stations should be higher than the CIMO standard.

(3) Both observation and simulation show that water body can lower the temperature of the surrounding areas in the downwind direction during the day, but increase temperature there over night. The significant impact is observed at the site 100 m away from water body, and it can increase by 1.7℃ at night and drop by 1.3℃ in the day at most. Simulation also shows that, in the 200 m range, there is 0.1℃ temperature decrease in the day and more than 0.05℃ temperature increase at night. The simulation values are lower than the observations in general, but the impact scopes are simulated more clearly.

(4) Both observation and simulation denote that the 0.1℃ impact range in the surrounding area of the downwind direction caused by 10 m wide road can get to 100 m. Simulation reveals that the impact range of road under light wind background condition is larger than under high wind background and the biggest impact range is seen when the wind speed is 2 m/s. Broadening the road to 30 m can make the 0.1℃ impact range extend to 120 m.

(5) Observation suggests that the temperature observed by stations at Grade 4 is obviously higher than by the stations in Grade 2-3 and the biggest difference can reach 0.3℃. The increasing temperature effect is more clearly seen at night than during the day. Regarding simulation to this effect, better methods are not obtained yet.

Reference

World Meteorological Organization, *Guide to Meteorological Instruments and Methods of Observation* (2010 version)